International Dairy Journal 169 (2025) 106338

Contents lists available at ScienceDirect

International Dairy Journal

journal homepage: www.elsevier.com/locate/idairyj

Research paper

Microfiltration of skim milk using hollow fiber membranes: Impact of membrane length, crossflow velocity and diafiltration cycles

Hilda Lucy Nyambura [a,*], Anja E.M. Janssen [a], Remko M. Boom [a], Albert van der Padt [a,b]

[a] Food Process Engineering Group, Wageningen University & Research, P.O. Box 17, Wageningen, 6700AA, the Netherlands
[b] FrieslandCampina, Stationsplein 4, 3818 LE, Amersfoort, the Netherlands

ARTICLE INFO

Keywords:
Diafiltration
Casein micelle layer
Hollow fiber
Serum protein removal
Casein recovery

ABSTRACT

This paper investigates the casein - serum protein fractionation efficiency during both the concentration and diafiltration using hollow fiber membranes and reverse osmosis water at 10 °C and the effect of membrane length and crossflow velocity. Membrane module length had no effect on flux and transmission and flux increased with increasing crossflow velocity with no effect on transmission, as the sieving layer made up of casein remained unchanged. Diafiltration at volume reduction factor of 2.5 at 0.5 bar transmembrane pressure gave the highest serum removal. Further diafiltration above three diafiltration cycles is not desired as the purity of the serum protein gets compromised. Usage of reverse osmosis water as the diafiltration medium achieves high serum removal even though it induces structural changes of the concentration polarization layer. Finally, this study verifies that hollow fiber membranes can be used effectively in the dairy industry where reverse osmosis water is the main diafiltration medium.

1. Introduction

In the dairy industry, fractionation of skim milk into casein and serum protein via microfiltration is gaining interest. Both ceramic tubular (CTM) and spiral wound membranes (SWM) are state of the art pertaining to skim milk fractionation (Hartinger, Heidebrecht, et al., 2019; Samuelsson, Dejmek, et al., 1997; Samuelsson, Huisman, et al., 1997; Schopf et al., 2020, 2021; Vadi & Rizvi, 2001; Zulewska & Barbano, 2013; Zulewska et al., 2009). SWM offer higher packing density and are inexpensive compared to CTM (Hartinger, Heidebrecht, et al., 2019; Schopf et al., 2021). On the other hand, SWM are more susceptible to fouling due to the presence of spacers that act as a divider between the membrane layers that are wound together to form a module (Beckman & Barbano, 2013; Hartinger et al., 2020; Hartinger, Heidebrecht, et al., 2019). CTM are highly resistant to thermal and chemical stresses and have effective fouling control (Schopf et al., 2021), but they have low packing density, are expensive and their brittleness complicates their handling (Zulewska et al., 2009). As an alternative, hollow fiber membranes (HFM) have previously been applied in drinking and waste water treatment and in the food industry for the production of beverages (Yeh, 2009). In the recent years, HFM have started to gain popularity in the dairy industry, as they have high membrane surface area packing density compared to CTM and allow better fouling control during filtration compared to SWM (Carroll & Booker, 2000; Li et al., 2017; Schopf et al., 2020, 2021).

In crossflow mode the separation characteristics and fouling typically depend on the length of the membrane. This is caused by the pressure drop along the length of the module. Schopf et al. conducted a study on the impact of the membrane length on milk protein fractionation at 55 °C using HFM (Schopf et al., 2020). Four membranes with a length of 0.32 m were arranged in series and other lengths of 0.32, 0.62, and 1.22 m were investigated using a variety of crossflow velocities. The optimal length to achieve substantial flux and low transmembrane pressure was 0.6 m (Schopf et al., 2020). Piry et al. studied the influence of the fiber length on flux and permeation of milk protein during microfiltration of skim milk using CTM at 55 °C. Their membrane module contained four sections of CTM of 29.5 cm, arranged in series (Piry et al., 2008). They found that flux was constant up to a length of 75 cm and declined above that. The beta-lg permeation increased with increasing length because the last section in the series experienced the least amount of fouling hence low filtration resistance as compared to the first three sections. At the first three sections, the concentration polarization layer is more compact and has lower porosity and higher resistance against protein permeation (Piry et al., 2008). The optimum

* Corresponding author.
E-mail address: hilda.nyambura@wur.nl (H.L. Nyambura).

https://doi.org/10.1016/j.idairyj.2025.106338
Received 16 February 2025; Received in revised form 11 June 2025; Accepted 21 June 2025
Available online 21 June 2025

should therefore be formulated as a function of flux and serum protein transmission. The length-wise adjustment of the transmembrane pressure using SWM was investigated at 10 °C by Hartinger, Schiffer, et al. (2019). The membrane was divided into four sections of 0.24 m in length. The permeate flux was within the limiting region up to a length of approximately 0.65 m above which the flux decreased. The permeation of serum protein, however, increased with the increasing length of the membranes. By ensuring that all the sections have the same transmembrane pressure, the filtration performance could be improved to be similar to those of CTM (Hartinger, Schiffer, et al., 2019). Above studies show that the filtration process with SWM, HFM and CTM is controlled by the fouling layer on the membrane surface on the first three sections that increases the filtration resistance. However, the last section had such a low transmembrane pressure that it operated below the critical flux and hence was deposit controlled and not pressure controlled.

The ideal module length strongly depends on the transmembrane pressure experienced at each point of the membrane length for a given crossflow velocity. This has a strong impact on the efficiency of the fractionation process. Therefore, investigating the effect of length during cold microfiltration (10 °C) is necessary to observe the differences and similarities with the abovementioned studies. Since, filtration at 50 °C induces some level of beta-lactoglobulin denaturation up to 5 %, cold microfiltration is beneficial as the nativity of the protein is guaranteed. Additionally, higher temperature results in the modification of the concentration polarization layer in terms of porosity due to intense interaction of proteins caused by folding and unfolding of proteins hence limiting the operation time. Decrease in porosity of this layer is also caused by precipitation of calcium phosphate on the membrane surface. On the other hand working at cold microfiltration aids in production of beta casein enriched serum protein stream and process stability in terms of flux hence allowing for longer processing times (Crowley et al., 2015; France et al., 2021; Steinhauer et al., 2015). In skim milk, beta casein represents 35 % of the total casein in milk and exists in the micelle as it associates with other fractions of caseins through hydrophobic interactions (De Kruif & Holt, 2003). This hydrophobic interaction strength is reduced when the temperature is lowered resulting in dissociation of beta casein into the serum phase of skim milk (France et al., 2021). Hence fractionation of skim at lower temperatures has increased interests especially in making the infant formula. Establishment of the optimal length paves way for the next step. This step includes incorporation of concentration and diafiltration of skim milk to improve the efficiency of the process. To operationalize these findings on membrane length, and quantify the efficiency of the filtration process, incorporation of diafiltration process in the overall process design is beneficial. This is because at the end of the process, serum protein removal and purities can be calculated as they are some of the performance indicators of the process.

There are four types of diafiltration: intermittent feed diafiltration, constant volume diafiltration, variable volume diafiltration and constant volume-to-concentration ratio diafiltration (Song et al., 2021). Intermittent feed diafiltration and continuous volume diafiltration are the most used configurations. Intermittent feed diafiltration involves adding a known volume of diafiltration medium to an already pre-concentrated feed and then removing this volume again as permeate. For continuous volume diafiltration, the diafiltration medium is added at the same rate as the permeate flow rate (Song et al., 2021). The choice of diafiltration medium plays a significant role during diafiltration. Using permeate from milk ultrafiltration (PUF) has been investigated by different researchers and its efficiency established. PUF ensures that the feed ionic strength during filtration remains constant hence the structure and integrity of the casein micelles is maintained thus the concentration polarization layer does not change (Dalgleish & Corredig, 2012; Gaucheron et al., 1997; Gebhardt et al., 2005; Renhe et al., 2019). Schopf and Kulozik (2021) determined the effect of the concentration level and diafiltration on skim milk fractionation at lower temperatures of 10 °C using HFM. They used continuous diafiltration mode and PUF as the diafiltration medium. Upon increasing the concentration level, the concentration polarization layer on the membrane progressively started hindering the flux. If this layer is further compacted and compressed by application of higher transmembrane pressures, the serum protein transmission reduces (Schopf & Kulozik, 2021). This is because the porosity of the concentration polarization layer is reduced by the compaction and since filtration of milk proteins is size exclusion driven, the reduced pore sizes in the concentration polarization layer hinders the transport of serum proteins. Schopf and Kulozik showed that the optimal concentration factor is 2.5 when the process is operated at 0.5 bar transmembrane pressure and 1.0 bar pressure drop.

However, water is the most common diafiltration medium used in the dairy industry. This has been investigated using CTM and SWM at 50 °C and 24 °C respectively using Reverse Osmosis (RO) water as the diafiltration medium and in intermittent diafiltration mode (Marella et al., 2021; Mercier-Bouchard et al., 2017; Tremblay-Marchand et al., 2016). These three studies reported an increase in permeate flux, serum protein removal and purity of casein in retentate with more diafiltration cycles. Reitmaier et al. (2021) investigated the effect of different diafiltration media (PUF, RO water, tap water, and softened water) on casein micelle characteristics, concentration polarization layer properties and separation properties during milk fractionation. Here CTM at operation temperature of 50 °C was used. The results showed an increase in flux levels and separation due to the hydration of the concentration polarization layer with RO water (Reitmaier et al., 2021). Tap water and softened water induced the least changes on the concentration polarization layer due to higher ionic strength as compared to RO water. Since, these studies were conducted under higher temperature conditions, similar investigations to ascertain whether there is transferability of results to common applications with HFM is crucial to the dairy sector. Further, Granger-Delacroix et al. (2023) studied the impact of using PUF and RO water on the concentration polarization layer and the resulting effect on both flux and transmission using SWM at 12 °C. Fluxes increased when RO water was used due to the decrease in permeate viscosity and ionic strength. The transmission of serum protein increased with an increasing rate of diafiltration at the beginning of the diafiltration process but decreased after a maximum was reached. This is linked to changes in the concentration polarization layer due to the change in structure of the casein micelles (Granger-Delacroix et al., 2023). This study was conducted using continuous diafiltration, which aims at minimizing membrane area and filtration time. Intermittent diafiltration is more suitable for minimizing the required diafiltration media volume. There exist a knowledge gap on studying the efficiency of HFM when operated in intermittent mode of diafiltration at 10 °C with reverse osmosis water. Since the operation kinetics are different in HFM and SWM, the results on HFM are a crucial contribution to understand how the different diafiltration mode, lower temperature and membrane configuration play a role in serum removal and the purity of the end product.

We therefore aim to demonstrate the role of the concentration polarization layer on the membrane in governing the filtration of milk proteins and examining the effects of varying lengths of hollow fiber membranes at low temperatures. This study aims to demonstrate that use of different membrane configuration (hollow fiber) for fractionation of skim milk in intermittent diafiltration mode using reverse osmosis as the diafiltration media yields significant serum protein removal.

2. Material and methods

2.1. Materials

Pasteurized skim milk was sourced locally from FrieslandCampina BV, The Netherlands, through one of their distributors (Jumbo Supermarket). The milk was stored at a temperature of 4 °C before the experiments (up to four days). All experiments of skim milk fractionation were performed at 10 °C and at a pH of 6.8.

The hollow fiber membranes were provided by Pentair-X-Flow, Enschede, The Netherlands. The membranes are made of polyethersulfone (PES) with a nominal pore size of 0.1 μm and an inner and outer diameter of fibers of 1.5 mm and 2.35 mm respectively according to the manufacturer's specifications for all the membrane modules used. These membranes are operated in inside-out filtration mode where the feed flows inside the fiber and the permeate is collected on the outside. Two types of membrane modules were used: one with a length of 300 mm and the other of 750 mm (see Supplementary materials Fig. S1). In each module, forty fibers were enclosed in a polysulfone (PSU) tube, with the entrance and the exit of the modules covered in potting of approximately 25 mm length. Potting refers to the process of glueing together fibers in a module using an adhesive to maintain intactness and strength of the module. Due to this process, the length of the fiber glued together does not contribute to the active membrane filtration area.

2.2. Membrane filtration system

All experiments were performed using a pilot scale filtration unit which was equipped with a frequency regulated centrifugal pump (CSF Inox, Montecchio E. Italy) (see Supplementary materials Fig. S1). The temperature was controlled by a double-walled feed tank connected to a heat exchanger that circulated temperature-controlled water through the tank jacket. The feed and permeate temperatures were recorded using a temperature probe in the feed tank and in line at the exist of the permeate from the module respectively. The retentate temperature is not measured as is recirculated back to the feed tank. The pressures of the feed, retentate and permeate were registered using digital pressure transmitters (Cerabar T, Endress and Hauser, Germany). The flow volume was registered using volume flow meters (Es-Flow, Bronkhorst, UK).

2.3. Conditioning and cleaning procedures

After each filtration experiment, the membrane module and the pilot unit were cleaned separately. The membrane module was cleaned with an enzymatic agent (0.3 % v/v Ultrasil 67, Ecolab Deutschland GmbH, Germany) and a caustic agent (0.1 % v/v Ultrasil 69, Ecolab Deutschland GmbH, Germany) at 50 °C for 40 min. Finally, an acidic agent (HNO3 at a pH of 2) was used at 50 °C for 35 min. The pilot unit was rinsed with water and then cleaned with caustic (NaOH 33 % v/v) at 50 °C. Finally, all water in the system was flushed out using pressurized air. Before starting any experiments, the membrane modules were rinsed with reverse osmosis water for 15 min and their clean water flux was checked to ensure that the membrane modules were thoroughly cleaned. To ascertain the cleanability of the membrane module, the clean water flux after every cleaning cycle is checked against the initial clean water flux of the new membrane. If the difference was less than 10 %, the membrane was considered clean (see Table S2 in supplementary materials). If this was not achieved a second cleaning cycle was performed.

2.4. Experimental design

All experiments were performed in duplicate using different batches of milk. At the start of filtration, the milk was conditioned to 10 °C in the feed tank for 20 min after which the filtration was started at given crossflow velocity and transmembrane pressure. During the experiments, pressures (feed, retentate, and permeate pressure), permeate flow rate, crossflow velocity and temperature were monitored and controlled using a control software. Three different filtration protocols were adopted.

2.4.1. Filtration at different crossflow velocities

Using the two different module lengths, four crossflow velocities were investigated: 0.5, 1, 1.5, and 2 ms^{-1}. In these experiments the pressure drop changed as the crossflow velocity and length increased. The experiments were conducted in batch mode with total recirculation of permeate and retentate stream into the feed tank.

2.4.2. Filtration in concentration mode

With the 300 mm module, the crossflow velocity was kept constant at 1.5 ms^{-1} and the milk recirculated in the system for 30 min to achieve steady state. The milk was then concentrated by draining the permeate stream to achieve a specified volume reduction factor (VRF - two and three) from known initial feed volume (V_{feed}) to a final volume of the retentate at the end of concentration ($V_{end\ of\ concentration}$). We carried the experiments out at 0.5 bar transmembrane pressure over a period of not less than 5 h taking samples every hour. Some experiments were extended over longer times to assess the stability over extended periods of time.

2.4.3. Filtration in diafiltration mode

Skim milk was pre-concentrated at a constant crossflow velocity of 1.5 ms^{-1} using the 750 mm module. After the concentration step, diafiltration was performed on the concentrated milk in intermittent diafiltration mode. RO water was used as a diafiltration medium and was added to the concentrated retentate in a volume equal to the amount of permeate drained to achieve a given VRF. The mixture of RO water and concentrated milk was then recirculated in the filtration loop for 30 min for effective mixing and to achieve steady state. After achieving a steady state, a permeate volume equal to the amount of RO water added was then drained and the cycle was repeated four times. Each of these cycles is referred to as a diafiltration cycle (DF cycles).

During all the above experimental routes, retentate and permeate samples were taken for further analysis using High Performance Size Exclusion Chromatography (HPSEC)

2.5. Milk proteins determination

The analysis of casein and serum protein was done using High Performance Size Exclusion Chromatography (HPSEC), using two columns in series namely TSK G400SWxl 7.8 × 300 mm, 8 μm and TSK 53000SWxl 7.8 × 300 mm, 5 μm by Tosoh Bioscience. The mobile phase applied in an isocratic mode consisted of 0.01 % Trifluoroacetic acid (TFA) in 69.9 % High Performance Liquid Chromatography (HPLC) grade water and 30.0 % Acetonitrile (ACN). The flow rate was 1.5 ml/min, the column temperature was kept at 30 °C and detection was done at a UV wavelength of 215 nm. For the analysis of the serum proteins, the casein was precipitated by adding 4 M hydrochloric acid and centrifugating at 4000 g for 10 min. The supernatant was then analyzed using the abovementioned columns, eluents, and operation conditions. HPLC calibration curves were made using casein and serum protein standards that aided in calculation of the actual concentration of casein and serum protein in skim milk, retentate and permeate samples (see supplementary materials Figs. S2 and S3).

2.6. Calculation of characteristics of microfiltration process

The flux, $J\ \left(Lm^{-2}h^{-1}\right)$, is calculated as a function of the permeate flow rate $Q_{perm}\ \left(lh^{-1}\right)$ and the active membrane area, $A_{mem}\ \left(m^2\right)$ as Equation (2.1):

$$J = Q_{perm} / A_{mem} \tag{2.1}$$

The (average) transmembrane pressure (bar) used was calculated as Equation (2.2):

$$Transmembrane\ Pressure\ (TMP) = \left(P_f + P_r \,/\, 2\right) - P_p \tag{2.2}$$

Where P_f, P_r, and P_p are feed, retentate and permeate pressures (bar).

The pressure drop (Δp_l) (bar) over the length of the membrane module was calculated as the difference between P_f and P_r. Additionally, the wall shear stress (τ_w (Pa)) experienced was calculated as a function of the active length of the membrane (L (m)), inner diameter of the fibers (d (m)), and the pressure drop (Δp_l (bar)) as in Equation (2.3):

$$P_f - P_r = \Delta p_l = \tau_w 4L/d \tag{2.3}$$

The thickness of the concentration polarization layer ($\delta\,(m)$) is calculated using the following Equation (2.4) where Re is the Reynolds number, Sc is the Schmidt number equal to 3.36 x 10^6, x (m) is the axial distance of the fiber, and d (m) is the inner diameter of the fibers. In this case the concentration polarization layer includes also the deposit layer that is mainly made up of casein micelles (Wang et al., 2017).

$$Sh = 1.62Re^{0.33}Sc^{0.33}(x/d)^{-0.33} = d\Big/\delta \tag{2.4}$$

The resulting mass transfer coefficient (k (ms^{-1})) can be calculated using Equation (2.5) where Sh is the Sherwood number, d (m) is the inner diameter of the membrane fiber, δ (m) is the thickness of the concentration polarization layer, and D $(m^2 s)$ is the casein diffusion coefficient equal to 6.9 x 10^{-13} m^2s^{-1} (Kattan et al., 2018; Rizki et al., 2019; Wang et al., 2017).

$$Sh = d/\,\delta = kd/D \tag{2.5}$$

The transmission of milk protein i (T_i (%)) was determined as a function of the protein concentration in the permeate ($C_{i,permeate}\left(gl^{-1}\right)$) and retentate ($C_{i,retentate}\left(gl^{-1}\right)$) as Equation (2.6):

$$T_i = C_{i,permeate}\big/C_{i,retentate} \times 100 \tag{2.6}$$

The volume reduction factor (VRF) was calculated as the ratio of the initial feed volume (V_{feed} (l)) and the final volume after concentration ($V_{end\ of\ concentration}$ (l)) as Equation (2.7):

$$VRF = V_{feed}\big/V_{end\ of\ preconcentration} \tag{2.7}$$

The mass flow of protein i $\left(gm^{-2}h^{-1}\right)$ was calculated as a function of the permeate concentration in the permeate ($C_{i,permeate}$ $\left(gl^{-1}\right)$) and the flux (J $\left(Lm^{-2}h^{-1}\right)$)experienced by the membrane at a specific trans-membrane pressure of evaluation as Equation (2.8):

$$M_{flow} = C_{i,permeate} \times J \tag{2.8}$$

The absolute decrease in protein concentration (X) in the retentate during the diafiltration process was defined as a percentage of the ratio of the concentration of a specific protein at a given diafiltration cycle ($C_{i,DF=n}$ $\left(gl^{-1}\right)$) and concentration of the same protein after concentration prior to the addition of diafiltration water ($C_{i,DF=0}$ $\left(gl^{-1}\right)$) (Schopf & Kulozik, 2021) as Equation (2.9).

$$X = C_{i,DF=n}\big/C_{i,DF=0} \times 100\% \tag{2.9}$$

The filtration time (t (h)) required to achieve one diafiltration cycle at a target concentration level is defined according to Equation (2.10) (Asbi & Cheryan, 1992; Cheryan, 1998).

$$t = V_{permeate}\Big/\left(A_{mem} \times J_{average}\right) \tag{2.10}$$

$$J_{average} = J_{initial}/3 + 2J_{final}/3 \tag{2.11}$$

The purity of the protein in the permeate for serum protein and in the retentate for casein was calculated with Equation (2.12):

$$Purity = C_{i,permeate\ or\ retentate}\big/C_{all\ proteins\ in\ permeate\ or\ retentate} \times 100 \tag{2.12}$$

The yield of milk proteins in the permeate was calculated as a function of the volume of feed (V_{feed} (l)), volume of permeate ($V_{permeate}$ (l)),concentration of in the permeate ($C_{i,permeate}\left(gl^{-1}\right)$) and feed ($C_{i,feed}$ $\left(gl^{-1}\right)$). Yield was calculated for all components i and n represents the number of cycles (concentration and diafiltration cycles).

$$Yield = \sum_{0}^{n} V_{permeate}C_{i,permeate}\Bigg/V_{feed}C_{i,feed} \times 100 \tag{2.13}$$

Membrane resistance (R_{tot}) was calculated as a function of trans-membrane pressure (TMP, (Pa)), viscosity (μ (Pa.s), and flux (J $(m^3m^{-2}s^{-1})$) as shown in equation (2.14).

$$R_{tot} = TMP/_{\mu} \times J \tag{2.14}$$

2.7. Data analysis and statistical significance determination

The software package Origin 2023b (OriginLab Corporation, Northampton, Massachusetts, United States) was used for analysis. Analysis of variance (ANOVA) combined with Tukey's test was used to determine whether differences in a particular set of measured parameters were statistically significant. Data shown are averages of the results obtained from two independent filtration experiments with error bars showing the absolute difference between two sets of experiments.

3. Results and discussion

3.1. Effect of crossflow velocity on flux and protein transmission

Different crossflow velocities from 0.5 ms^{-1} to 2 ms^{-1} with 0.5 ms^{-1} intervals were used in a 300 mm module. For each crossflow velocity, the transmembrane pressure was varied from 0.2 bar to 1 bar. The flux, protein transmission and component mass fluxes were evaluated. Fig. 1 (left) shows that the permeate flux increases with the increase in crossflow velocity. This increase in crossflow velocity improves the hydrodynamic conditions near the membrane surface such as shear stress further positively increasing the permeate flux. The permeate fluxes shown are independent of the increase in transmembrane pressure indicating that at 0.2 bar the critical transmembrane pressure is already reached, and a stagnant layer of casein micelles has been formed on the membrane surface. This shows that 0.2 bar is a sufficient trans-membrane pressure for operation, as further increase does not result in any significant increase in permeate flux but will lead to further accumulation of proteins on the membrane.

Fig. 1 (right) shows that permeate flux plotted versus the Reynolds number (Re). We can conclude that the flow regime is laminar as the flux can be described by the relation $Flux = a\,Re^{0.5}$ where a = 0.967. At the highest value of Re used, we observed that the flux measured develops a higher slope than 0.5 (Montagnaro, 2024). This indicates that the regime is transitioning to a turbulent regime. This transition happens when the Re = 1200 in tubes which is equivalent to the Re for the highest permeate flux measured during filtration. The pressure drop over the length of the module experienced with 300 mm module ranged from 0.07 to 0.3 bar with 0.5 ms^{-1} and 2.0 ms^{-1} crossflow velocity, respectively.

Equation (2.4) has been used to calculate the concentration polarization layer thickness (see Supplementary Material Fig. S4). This layer is expected to be mainly made up of casein micelles (Doudiès et al., 2021; Nyambura et al., 2025). At 0.5 ms^{-1}, its value is two times higher than that of 2.0 ms^{-1} (5.6×10^{-5} m versus 1.2×10^{-4} m). This means that there is a loss of fiber diameter by 0.24 mm at 0.5 ms^{-1}, while at 2.0 ms^{-1}, the loss of fiber diameter is only 0.12 mm. A higher crossflow velocity increases the mass transfer by reducing the thickness of the concentration polarization layer on the membrane, allowing for higher fluxes. The mass transfer coefficient at 0.5 ms^{-1} is two times smaller $\left(6.0\times10^{-9}\ ms^{-1}\right)$ as compared to that at 2.0 ms^{-1} $\left(1.2\times10^{-8}\ ms^{-1}\right)$. The reduction in the thickness of the concentration polarization layer on the membrane surface is also due to increase in shear stress with increase in crossflow velocity (τ_w at 2.0 ms^{-1} = 45 Pa versus τ_w at 0.5 ms^{-1} = 11 Pa) (Equation (2.3)) as shear stress increases with increase in crossflow velocity (Berre & Daufin, 1996; Holdich et al., 2018).

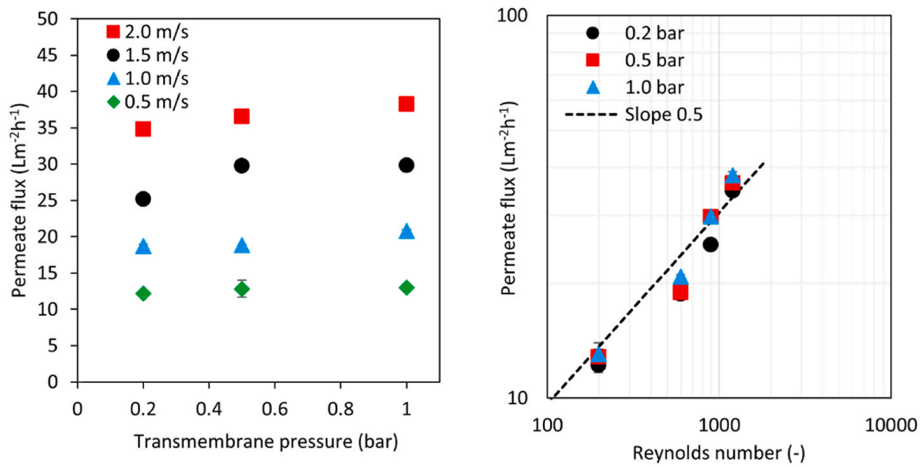

Fig. 1. Effect of varying crossflow velocity on permeate flux. The permeate flux is plotted versus the transmembrane pressure at various crossflow velocities (left). The permeate flux is also plotted versus the Reynolds number at various transmembrane pressures (right). The graph on the right is fitted with a line that has a slope = 0.5. The experiments were performed using a 300 mm long hollow fiber membrane module (for experimental design, see section 2.4.1). The Reynolds number is calculated by using equations (2.3)-(2.5). The error bars are very small and might be obscured by the symbols.

The transmission of beta-lg was highest at 0.2 bar, and decreased at higher transmembrane pressures, as shown in Fig. 2 (left) for each crossflow velocity investigated (Equation (2.6)). At lower transmembrane pressures, the thickness of the concentration polarization layer made up of majorly casein micelles is smaller but increases as the transmembrane pressure is increased. At elevated pressures, the casein micelles are squeezed onto each other, leaving smaller interstitial pores between them for dissolved proteins to permeate through, lowering their transmission (Nyambura et al., 2025; Tan et al., 2014). The reduction in porosity of the polarization layer also increases the filtration resistance (Piry et al., 2008) hindering the transport of proteins through this layer. This is due to these proteins being in the same order of size compared to the interstitial pores present in the concentration polarization layer since filtration of dairy proteins is mainly due to size exclusion (Nyambura et al., 2025). Along the length of the membrane, the transmission of Beta-lg increases as the resistance of the casein concentration polarization layer reduces. This is because the porosity of this layer also increases along the membrane length since the compaction is reduced due to the local transmembrane pressure reducing along the membrane length (Piry et al., 2008; Schopf et al., 2020). Since our membrane was not divided in small sections, the flux could not be investigated as function of the axial position in the fibers, so the analysis on transmission is based on the average concentrations of serum proteins in the permeate and retentate. The same trend was observed with casein transmission.

Filtration performance is commonly evaluated by protein transmission, permeate flux and mass flow. However, evaluation of mass flux, calculated with equation (2.8), gives more insight into the effect of crossflow velocity. The amount of beta-lg permeated after an hour of filtration increased with increasing crossflow velocity and reduced with increasing transmembrane pressure as seen in Fig. 2.

3.2. Effect of length on flux and transmission

Fig. 3 (left) shows that the volumetric permeate flux differed only very slightly between these two membrane lengths for all the crossflow velocities indicated. The slight flux difference ranged from one to two $Lm^{-2}h^{-1}$ at all the crossflow velocities and membrane lengths investigated which was considered not significant (p value = 0.852). This indicates that with similar membrane properties and filtration conditions, the flux obtained with different membrane lengths is similar. It is worth noting that at 1 bar of transmembrane pressure for all crossflow velocity and membrane lengths investigated, the obtained permeate flux was the limiting permeate flux. This means that filtration is limited by the concentration polarization layer. Additionally, the shear stresses for both modules at different crossflow velocities were calculated to show their

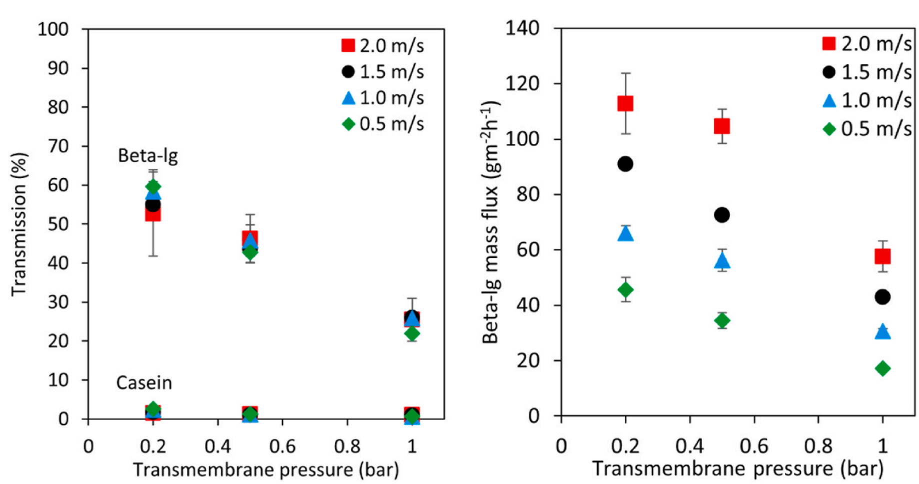

Fig. 2. Resulting transmission of beta-lg and casein (left) and beta-lg mass flux (right) when crossflow velocity was varied using 300 mm long hollow fiber membrane module (for experimental design, see 2.4.1). The error bars are very small and might be obscured by the symbols.

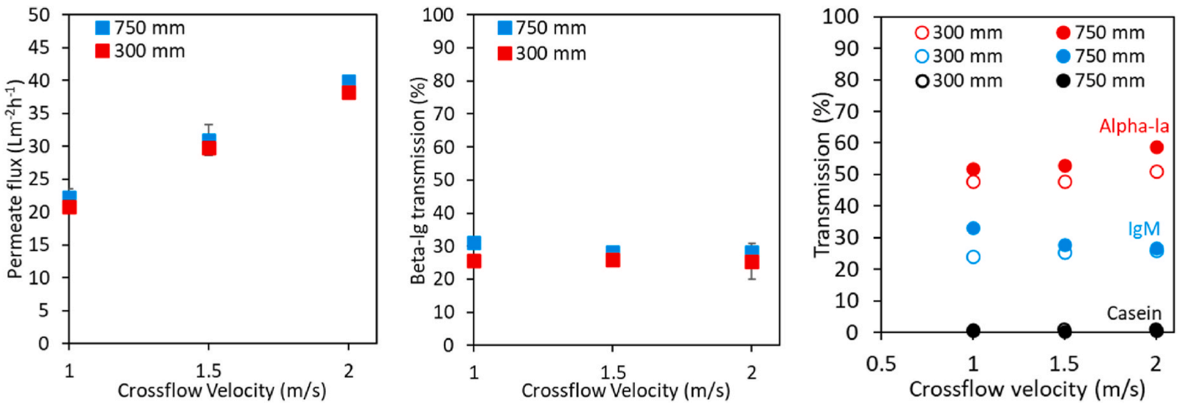

Fig. 3. Differences between 300 mm and 750 mm hollow fiber membrane modules in terms of permeate flux (left) and beta-lg transmission (middle) and alpha-la, IgM, and casein transmission (right)at different crossflow velocities. The transmembrane pressure used during these experiments was 1 bar (for experimental design, see 2.4.1). The error bars are very small and might be obscured by the symbols.

effect on the concentration polarization layer (Table 1). The shear stresses and the concentration polarization layer thickness for both long and short membrane modules were observed to be comparable with p values of 0.93 and 0.872 respectively (Table 1). The observation of decrease in concentration polarization layer with increase in crossflow velocity is validated using resistance of a fouled membrane where it decreases with increase in crossflow velocity. Schopf and Kulozik investigated the impact of the hollow fiber membrane length in fractionation of milk proteins at 55 °C and found that among the lengths they investigated (up to 1.2 m) the permeate flux was similar (Schopf et al., 2020). Equal permeate fluxes with lengths of up to 0.75 m were observed when CTM were used for the filtration of skim milk at 55 °C (Piry et al., 2008). Above 0.75 m, the permeate flux declined. Also, no change of permeate fluxes was observed up to a length of 0.65 m when SWM were used for the filtration of skim milk at 10 °C (Hartinger, Schiffer, et al., 2019). Above this length, the permeate flux declined. Thus, the flux and transmission behavior are both determined by the crossflow applied, and not by the characteristics of the specific membrane. A major difference observed was the lowest achievable transmembrane pressure. With the shorter module, a minimum transmembrane pressure of 0.2 bar could be achieved, while with the longer module, the minimum transmembrane pressure was 0.4 bar. This is due to the increase in friction and kinetic pressure loss experienced along the length of the membrane, which lead to very low pressure at the end of longer membrane fibers (Liang, 2016).

Fig. 3, (middle) shows the transmission of beta-lg was between 25 % and 30 % for both membrane modules. The transmission of alpha-la, IgM and casein had different values but followed the same trend (Fig. 3, right). Transmission of alpha-la was the highest due to the small size of the protein. The difference between the two modules was not considered significant as the transmission depends on the thickness and porosity of the casein concentration polarization layer and not on the length of the membrane. The p values for transmission of alpha-la, IgM and casein are 0.08, 0.3, and 0.11 respectively. On average both modules have similar performances as lower transmission expected at the entrance of the membrane is compensated by higher transmissions at the end of the membrane module as explained in Section 3.1.

3.3. *Effect of concentration on flux and transport of milk proteins through the membrane*

We observed a lower flux when increasing the VRF from 1 to 3 (Fig. 4 (left)). At higher VRF, the viscosity of the retentate increases, reducing the mass transfer through the concentration polarization layer, leading to more accumulation of casein on the membrane. At the same time, the advection of rejected components towards the membrane increases due to the larger bulk concentration. These two effects both reduce the flux.

To further evaluate the performance of this HF membrane at different VRFs, we assessed the concentration of milk protein in the retentate and permeate streams. Fig. 4 (right) shows decreasing transmission of serum proteins with increasing VRF. The transmission of casein is also decreasing as its values at VRF 1, VRF 2, and VRF 3 are 1.0 %, 0.5 %, and 0.4 %, respectively. This can be explained by the increasing size of the concentration polarization layer on the membrane with larger VRF. The increase in size of the concentration polarization increases the resistance hence lower transmission of casein. However, beta-lg still had a transmission above 30 %. The observed transmission was due to the porosity of the concentration polarization layer remaining constant. This porosity can be changed through compaction and compression, which is caused by the increase in pressure over the concentration polarization layer (Steinhauer et al., 2011). Since the transmembrane pressure was not changed during the experiment, the compression and compaction on this layer was assumed to be equal and constant.

The flux at VRF 2 with the 750 mm module was compared to that of the 300 mm module (Fig. 5). The difference between the two fluxes was only one $Lm^{-2}h^{-1}$, which was not considered significant (p value 0.96). Comparison on the performance of 750 mm module during

Table 1
Thickness of concentration polarization layer and wall shear stress calculated for different module lengths and crossflow velocity at a transmembrane pressure of 1 bar for both 300 and 750 mm module.

Crossflow velocity (ms^{-1})	Concentration polarization layer thickness (m)[1]		Wall shear stress (Pa)[2]		Membrane fouling resistance (m^{-1})[3]	
	750 mm	300 mm	750 mm	300 mm	750 mm	300 mm
1.0	8.2×10^{-5}	8.4×10^{-5}	21	20	6.75×10^{12}	7.44×10^{12}
1.5	6.6×10^{-5}	6.2×10^{-5}	32	36	4.84×10^{12}	5.36×10^{12}
2.0	5.7×10^{-5}	5.6×10^{-5}	43	45	3.76×10^{12}	3.93×10^{12}

1) The thickness of the concentration polarization was calculated using (equation (2.4)).
2) Wall shear stress was calculated using equation (2.3)).
3) Membrane resistance is calculated using equation (2.14).

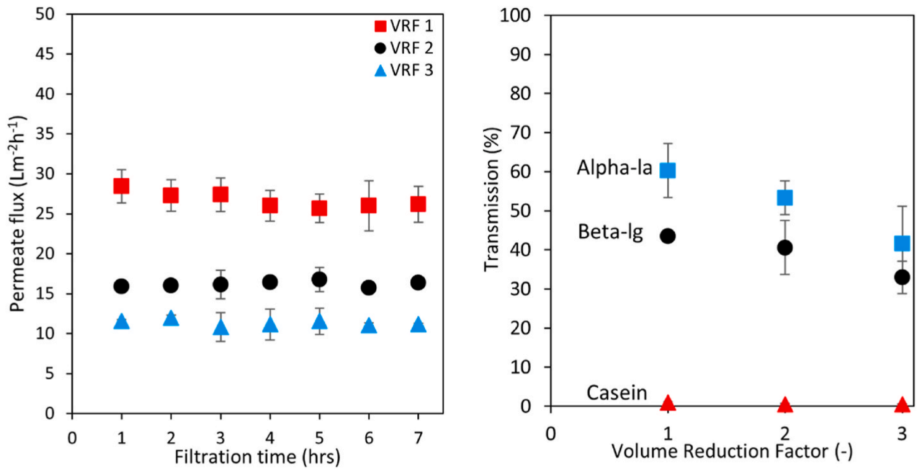

Fig. 4. (Left) Steady state permeate flux (with recycled permeate) after concentration of skim milk to different VRFs as function of the filtration time. (Right) Transmission of casein, beta-lg and alpha-la is shown with respect to varying VRFs. These experiments were conducted using a 300 mm long hollow fiber membrane with 1.5 ms^{-1} crossflow velocity and a transmembrane pressure of 0.5 bar (for experimental design, see section 2.4.2). The error bars are very small and might be obscured by the symbols.

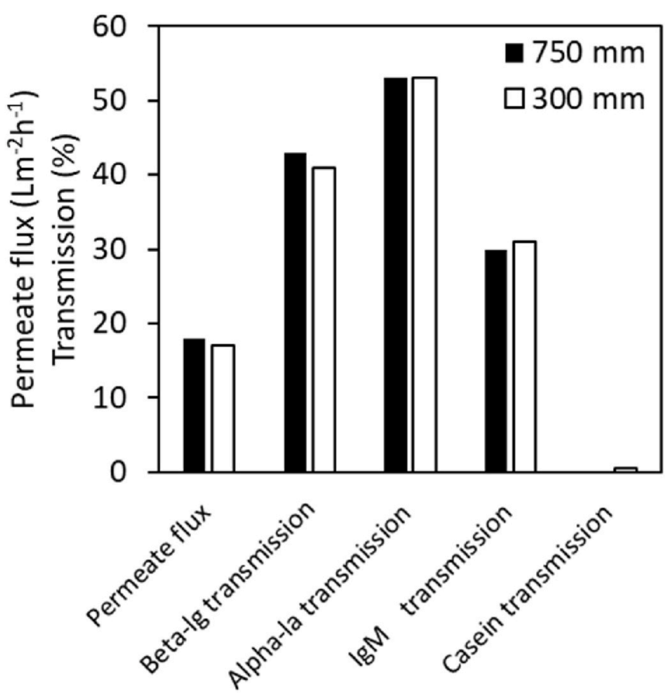

Fig. 5. Shows the differences between 750 and 300 mm modules during the concentration of skim milk to VRF 2 at 0.5 bar transmembrane pressure.

concentration to VRF 2 showed comparable results with p values of beta-lg, alpha-la, IgM and casein transmission being 0.55, 0.67, 0.1, and 0.68 respectively (Fig. 5). The transmission of casein, beta-lg and alpha-la was 0.2 %, 43 % and 53 % respectively. With the 300 mm module at VRF 2 the results were 0.5 %, 41 % and 53 % for casein, beta-lg and alpha-la, respectively.

Lastly, the mass flux of serum proteins was calculated by considering the concentration, partial depletion, and transmission of these proteins in the permeate stream for each VRF (equation (2.8)). The highest beta-lg mass flow of 35.3 $gm^{-2}h^{-1}$ but the differences between the mass fluxes of the three VRFs was minimal. Hence, the mass flux was considered constant (Fig. 6). It has been reported that after approximately VRF 3, further concentration of milk proteins in the feed does not improve the mass flow through the membrane (Schopf & Kulozik, 2021). This is due to the intense accumulation of proteins forming a dense concentration polarization layer that hinders the protein transport. This hindrance leads to less protein transport to the permeate. This could explain the decreasing trend in mass flow at VRF 3 compared to VRF 1 and 2. The small decrease of mass flow at VRF 3 could also be due to increased depletion of serum protein in the feed during the concentration stage from VRF 1 to 3, and lower flux. Schopf and Kulozik investigated concentration of skim milk using hollow fiber membranes at 10 °C and found that the optimum concentration factor was 2.5 (Schopf & Kulozik, 2021). This agrees with our results. Additionally, the increase in concentration of the proteins in the retentate as the concentration process continues, increases the concentration gradient in the concentration polarization layer. This results in the increase in the concentration of soluble proteins in the permeate stream that compensates for the decrease in permeate flux.

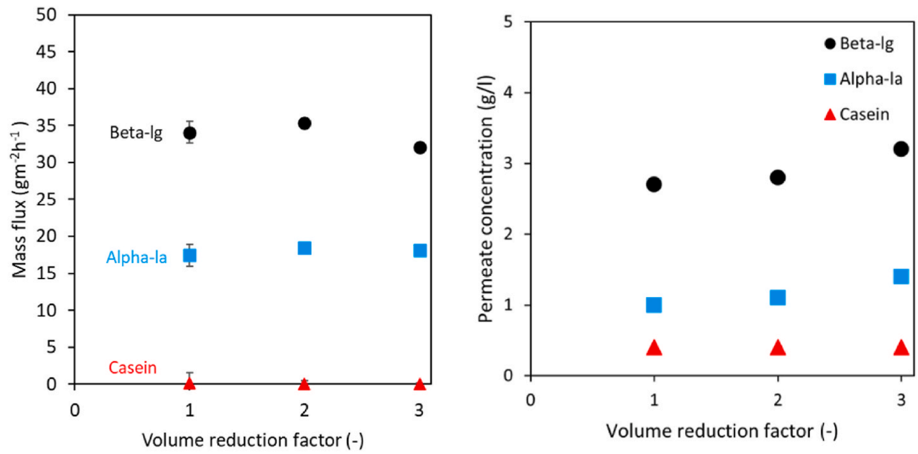

Fig. 6. Mass flux (right) (product of permeate concentration and permeate flux) at different VRF filtration was performed using 300 mm module at 0.5 bar transmembrane pressure and crossflow velocity of 1.5 m/s. Graph on the left show concentration of proteins in the permeate at each VRF.

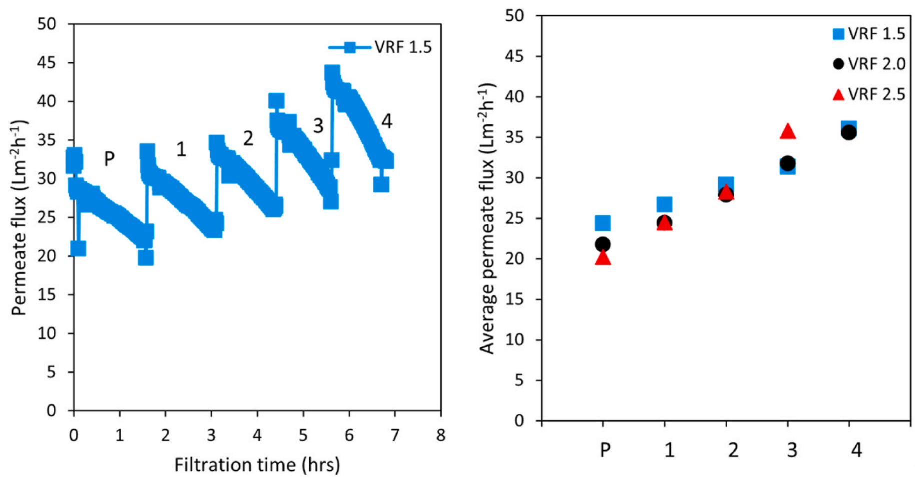

Fig. 7. Change in permeate flux with respect to the filtration time during one concentration (P) and four diafiltration cycles (1,2,3,4) and calculated average permeate flux (right) during concentration and different diafiltration cycles. Experiments conducted using 750 mm hollow fiber module at a crossflow velocity of 1.5 ms^{-1} (for the experimental design see section 2.4.3). The error bars are very small and might be obscured by the symbols.

3.4. *Effect of concentration on protein separation by diafiltration using RO water*

During concentration to different VRFs, the flux decreases in time (Fig. 7 (left)). This is due to the increase in viscosity and protein concentration in the retentate which results in a reduction of the diffusion coefficient and mass transfer coefficient (Song et al., 2021). At the end of the concentration step, a certain level of serum protein removal was achieved. To further remove the remaining serum protein in the concentrate, batch diafiltration was performed. Fig. 7 (left) shows that the permeate flux increased upon the addition of RO water due to the reduced viscosity. The same was observed with VRFs of 2 and 2.5 (see Supplementary Material Fig. S5). The reduced viscosity causes a reduction in hydrodynamic resistance of the concentration polarization layer. Upon the addition of the RO water, this layer is also disturbed and partially dispersed (Song et al., 2021). The permeate flux then again reduces over time as the concentration of the proteins in the retentate stream increases due to the removal of the permeate. From Fig. 7 (right), the average permeate flux is observed to have an increasing trend. This is due to the concentration polarization layer becoming increasingly thinner with each DF cycle. The composition of the concentration polarization layer and the retentate changes since the salts in milk were

Table 2
Overall yield, removal of serum proteins and purity of the retentate and permeate are shown for different VRFs combined with 3 diafiltration cycles using RO water.

	Serum Protein Removal (%)[1)]			Yield (%)[2)]			Mass ratio of casein: serum protein in permeate		Retentate Purity (%)
VRF	Beta-lg	Alpha-la	IgM	Beta-lg	Alpha-la	IgM	Casein	Serum protein	Casein
1.5	58	61	39	57	60	38	18	82	92
2	76	74	50	70	74	44	21	79	95
2.5	85	96	58	89	89	61	25	75	96

[1)] Serum protein removal is defined as the amount of serum protein removed from the initial feed volume of skim milk throughout the concentration and diafiltration process.

[2)] Yield is defined as the percentage of each specific protein obtained from the start of the concentration step to the end of the 3rd diafiltration step calculated using equation (2.13). Yield and serum protein removal are similar as seen from the numbers in the table hence in consensus with each other.

washed out by RO water during diafiltration (Granger-Delacroix et al., 2023). The resulting decrease in ionic strength may cause an increase in protein-to-protein repulsion in the concentration polarization layer, causing lower hydrodynamic resistance and higher fluxes (Ng et al., 2018). Our results are in agreement to those observed other researchers. Marella et al. (2021) observed an increase in permeate flux when diafiltration was performed at 150 % of the feed volume, at a concentration factor of three and a transmembrane pressure of 0.3 bar. Mercier-Bouchard et al. (2017), at concentration factor of three saw an increase in flux with two diafiltration cycles from 48.51 to 54.18 $kgm^{-2}h^{-1}$.

The goal of diafiltration is to further remove the serum protein from the micellar caseins. With three DF cycles, VRF 2.5 had the highest removal of beta-lg, alpha-la and IgM. It was also observed that the serum protein removal increased with increasing VRF (Table 2). The concentration step contributed to this increased removal of serum proteins. During this step, larger amounts of serum protein were removed at VRF 2.5 as compared to that at VRF 1.5 (see Fig. S6 (Left) in supplementary material). Hence, during the DF cycles the concentrations could drop even lower. The yield of the Beta-lg, alpha-la and IgM increased with increasing VRF with VRF 2.5 having the highest yield. The purity of the casein increased with increasing VRF, and with VRF 2.5 reaching 96 %. However, the mass ratio of casein to serum protein increased again at higher VRFs as seen in Table 2 as more diafiltration water was used and more casein permeated. This is supported by the decrease of purity of the serum proteins with increasing diafiltration cycles (see Fig. S6 (right) in supplementary material). The decrease in ratio of the serum protein mass with increase in VRF is due to the increase in concentration of casein in the permeate stream (see Fig. S9 in supplementary material). This observed high casein permeate concentration was due to the change in viscosity induced by use of RO water and also change in the concentration polarization layer thickness and chemistry (Mercier-Bouchard et al., 2017). On average, the permeate concentration of casein was 0.7 gl^{-1} which is low compared to its retentate concentration but is considered significant when compared to the concentration of serum proteins in the permeate. We compared our serum removal results with those of Marella et al. (2021) and found that they achieved 81.45 % removal of serum protein with 150 % diafiltration at lower transmembrane pressures of 0.3 bar. While our membrane configuration was different and lower temperature, we achieved significant alpha-la removal of 96 % with three diafiltration cycles.

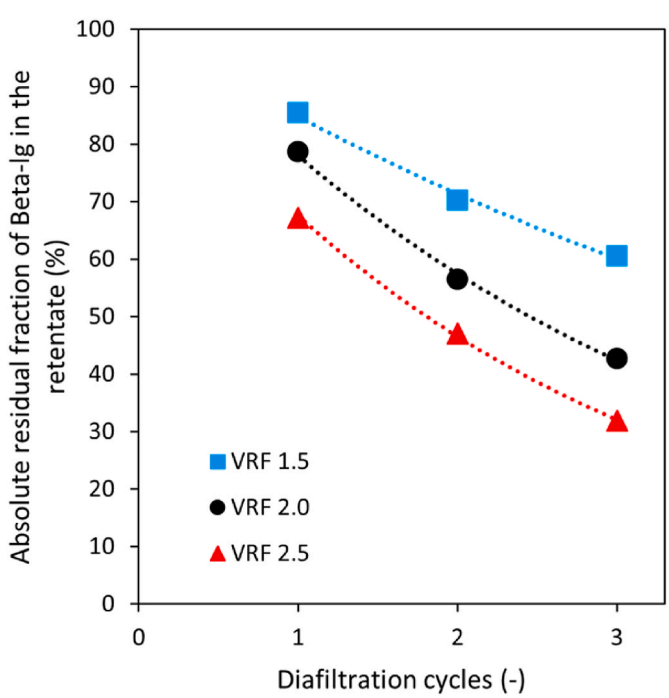

Fig. 8. Absolute residual fraction of Beta-lg in the retentate at different VRF and diafiltration cycles. The dotted lines on the graph on the right show an exponential relation in the decrease of the concentration of Beta-lg in the retentate. The error bars are very small and might be obscured by the symbols.

Table 3
The amount of diafiltration water required for the fractionation of 1000 L of skim with various diafiltration cycles and the R^2 score for the exponential relationship in the reduction of Beta-lg in the retentate. The number of calculated diafiltration cycles are similar since the behavior of retention with the three VRFs at the same diafiltration cycle is almost equal.

VRF	Volume of permeate per each step (Liters)	Number of diafiltration cycles	Diafiltration water (Liters) [(1)]	R^2 score [(2)]
1.5	334	29	9686	0.99
2.0	500	16	8000	1
2.5	667	13	8671	1

[1)] Diafiltration water that is needed to achieve the calculated diafiltration cycles when 1000 L of skim milk is fractionated using procedure outlined in Section 2.4.3. It is calculated as the volume of permeate multiplied by the number of diafiltration step.
[2)] R^2 score obtained from the linear relationship that is shown in Fig. 7.

Fig. 8 shows the decrease in concentration of Beta-lg in the retentate in comparison to the amount available after concentration to a known VRF. With only three diafiltration cycles, VRF 2.5 had the highest reduction of Beta-lg present in the retentate. This reduction was due to the higher removal of serum protein at VRF 2.5 during the concentration stage. There is an exponential decrease of the Beta-lg in the retentate during diafiltration with R^2 score shown in Table 3. The same relationship is observed with the decrease of alpha-la and IgM in the retentate (see Fig. S7 in supplementary material). This exponential decrease can allow for calculation of the concentration of serum protein in the retentate beyond the three diafiltration cycles. This relationship is helpful since due to the set-up limitations, diafiltration above three cycles for VRF 2.5 was impossible without affecting the integrity of the filtrate and the retentate. More than three diafiltration cycles are required to reduce the concentration of Beta-lg in the retentate to a minimum. To obtain a 99 % decrease in Beta-lg concentration in the retentate, VRF 1.5, 2.0 and 2.5 would require approximately 29, 16, and 13 diafiltration cycles respectively. See supplementary material (Table S1) for the calculation of the diafiltration cycles.

Such a high number of diafiltration cycles required to reduce the concentration of beta-lg in the retentate to 99 % warrants consideration of the amount of diafiltration media used. For that, we consider one thousand liters of milk to be fractionated using the procedure in section 2.4.3, with calculated number of diafiltration cycles. According to Table 3, VRF 1.5 would require the highest amount of diafiltration medium (9686 L) with VRF 2.0 having the lowest diafiltration medium consumption (8000 L). There is a slight difference between the amount of diafiltration water used for VRF 2.0 and VRF 2.5.

In addition to Table 3 and it is observed that the beta-lg removal improves as more diafiltration water is used but the purity of the casein in the retentate reduces. This would further imply that higher numbers diafiltration cycles are not necessary as the beta-lg removal would improve at the expense of its purity in the permeate. To further evaluate the ideal VRF and diafiltration cycles needed, we further plot the recovered beta-lg in the permeate against the recovered casein in the retentate.

As seen from Fig. 9, as the diafiltration cycles increase, the cumulative recovery of the beta-lg in the permeate increases but the cumulative recovery of casein in the retentate reduces. Change in cumulative total serum protein recovery in the permeate against cumulative casein recovery shows similar trend (see Supplementary Material Fig. S8). This is due to the increase in transmission of casein as more diafiltration water is applied. The ideal situation would be high recovery of casein in

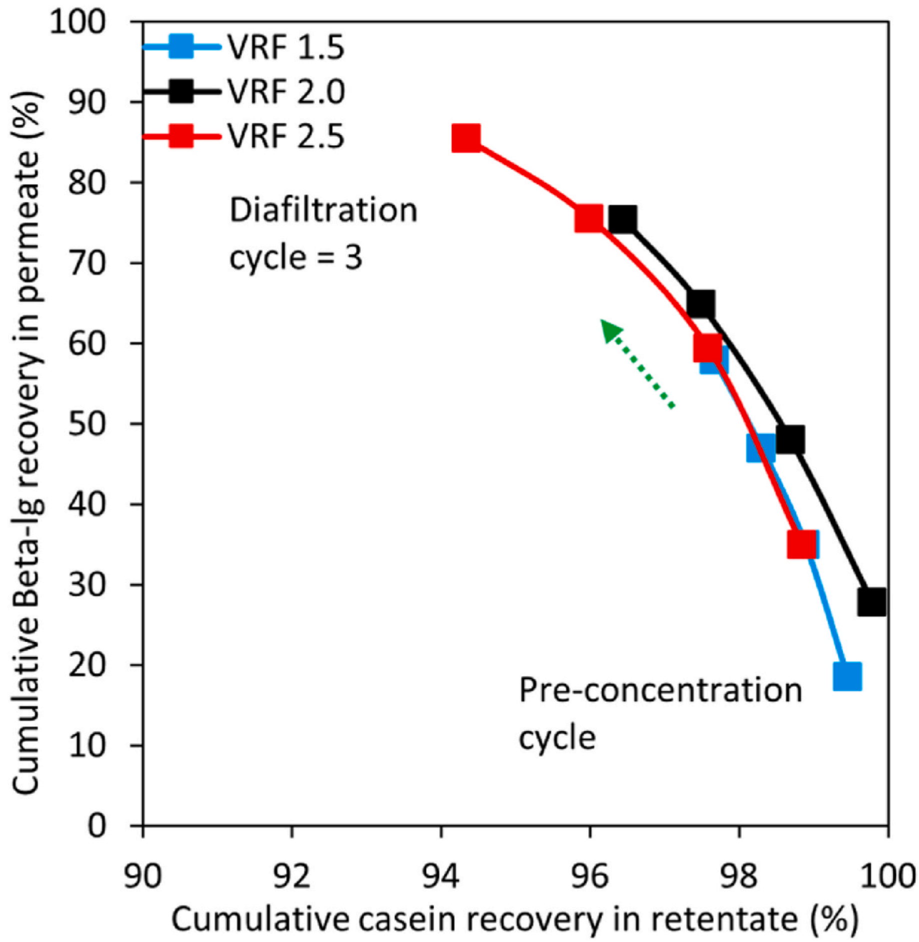

Fig. 9. The graph shows the relationship between the cumulative recovery of Beta-lg in the permeate versus the cumulative casein recovery in the retentate. The green dotted line points in the direction of the increase in the diafiltration cycles starting from the concentration phase to the last diafiltration cycle number three. The error bars are very small and might be obscured by the symbols. (For interpretation of the references to colour in this figure legend, the reader is referred to the Web version of this article.)

retentate and of beta-lg in the permeate. From Fig. 9, the ideal region for the outcome of a diafiltration process in terms of recovery of beta-lg in permeate and of casein in retentate would be on the top right hand side where both fractions are one. From these results VRF 2.0 at three diafiltration cycles yield the same results as VRF2.5 at two diafiltration cycles. Considering the purity of the permeate, VRF2.5 for two diafiltration cycles would be ideal since it has higher purity and less filtration time as compared to VRF2.0 at three diafiltration cycles. However, if more diafiltration cycles are to be used, further polishing of the permeate would be necessary to further remove casein present in permeate by using microfiltration membranes.

4. Conclusion

Fractionation of skim milk was performed using polymeric hollow fiber microfiltration membranes, to separate the serum proteins from the micellar casein. At 10 °C, we demonstrated that module length has no effect on flux and transmission since the filtration is controlled by the layer that accumulates on the membrane (during constant flux regime). These results depicted similar behavior that has been observed with CTM and HFM at higher temperature. Since the longer module (0.7 m) has higher permeate volume, it was used for concentration and diafiltration to reduce the filtration time. During fractionation, concentration is a key step in enhancing the removal of serum proteins from skim milk. A higher concentration at less diafiltration cycles results in more efficient serum protein removal and efficient recovery of casein. During diafiltration, RO water can be used to achieve high removal of serum protein since RO water is readily available and does not negatively affect the removal of serum protein.

The purity of serum protein reduces with more diafiltration cycles, since the diafiltration RO water washes out some of the casein to the permeate side over time. Addition of RO water affects the viscosity of the feed and the integrity of the micelles in the concentration polarization layer on the membrane surface due to the salts being washed out during diafiltration hence allowing casein to permeate through the membrane. Since the concentration polarization layer on the membrane surface acts as a dynamic filtration layer, minor changes in process conditions can result in major changes, such as the reduction of the serum purity with higher numbers of diafiltration cycles. The dynamic concentration polarization layer further rebuilds with each step, as the conditioning between each step allows for redispersion of the casein micelles that form the deposited layer. The combination of an optimal membrane length that saves on filtration time without compromising on permeate flux and transmission of serum proteins is a crucial first step that allows more diafiltration cycles to be applied. Higher number of diafiltration cycles allow for more removal of serum protein while minimizing on the membrane area required. The membrane area is minimized during intermittent diafiltration. Overall, intermittent diafiltration combined with concentration using HFM represents a viable substitute to fractionate serum proteins and casein.

CRediT authorship contribution statement

Hilda Lucy Nyambura: Methodology, Conceptualization, Writing – review & editing, Investigation, Writing – original draft, Formal analysis. **Anja E.M. Janssen:** Conceptualization, Writing – review & editing, Supervision. **Remko M. Boom:** Conceptualization, Writing – review & editing, Supervision. **Albert van der Padt:** Conceptualization, Writing – review & editing, Supervision.

Declaration of competing interest

The authors declare that they have no known competing financial interests or personal relationships that could have appeared to influence the work reported in this paper.

Acknowledgements

This publication is part of a project called 'Novel Process Routes (Reduction of Energy use by Novel process routes for food)' and is financially supported by the Institute for Sustainable Process Technology (ISPT) and TKI-E&I with the supplementary grant 'TKI- Toeslag' for Topconsortia for Knowledge and Innovation (TKI's) of the Dutch Ministry of Economic Affairs and Climate Policy. The author would like to thank all members of the ISPT Consortium for their contribution: Cosun, DSM firmenich, Friesland Campina, Nizo, Pentair, TU Delft and Wageningen University. More information can be found at https://ispt.eu/projects/novel-process-routes/. Click or tap if you trust this link.">https://ispt.eu/projects/novel-process-routes/.

Appendix A. Supplementary data

Supplementary data to this article can be found online at https://doi.org/10.1016/j.idairyj.2025.106338.

References

Asbi, B. A., & Cheryan, M. (1992). Optimizing process time for ultrafiltration and diafiltration. *Desalination, 86*(1), 49–62. https://doi.org/10.1016/0011-9164(92)80023-3

Beckman, S. L., & Barbano, D. M. (2013). Effect of microfiltration concentration factor on serum protein removal from skim milk using spiral-wound polymeric membranes. *Journal of Dairy Science, 96*(10), 6199–6212. https://doi.org/10.3168/jds.2013-6655

Berre, O. Le, & Daufin, G. (1996). Skim milk crossflow microfiltration performance versus permeation flux to wall shear stress ratio. *Journal of Membrane Science, 117*, 261–270. https://doi.org/10.1016/0376-7388(96)00076-2

Carroll, T., & Booker, N. A. (2000). Axial features in the fouling of hollow-fibre membranes. *Journal of Membrane Science, 168*(1–2), 203–212. https://doi.org/10.1016/S0376-7388(99)00319-1

Cheryan, M. (1998). *Ultrafiltration and microfiltration handbook* (2nd ed.). CRC Press. https://doi.org/10.1201/9781482278743

Crowley, S. V., Caldeo, V., McCarthy, N. A., Fenelon, M. A., Kelly, A. L., & O'Mahony, J. A. (2015). Processing and protein-fractionation characteristics of different polymeric membranes during filtration of skim milk at refrigeration temperatures. *International Dairy Journal, 48*, 23–30. https://doi.org/10.1016/j.idairyj.2015.01.005

Dalgleish, D. G., & Corredig, M. (2012). The structure of the casein micelle of milk and its changes during processing. *Annual Review of Food Science and Technology, 3*(1), 449–467. https://doi.org/10.1146/annurev-food-022811-101214

De Kruif, C. G., & Holt, C. (2003). Casein micelle structure, functions and interactions. *Advanced Dairy Chemistry, 1*(1), 233–276. https://doi.org/10.1007/978-1-4419-8602-3_5. Proteins 3.

Doudiès, F., Loginov, M., Hengl, N., Karrouch, M., Leconte, N., Garnier-Lambrouin, F., Pérez, J., Pignon, F., & Gésan-Guiziou, G. (2021). Build-up and relaxation of membrane fouling deposits produced during crossflow ultrafiltration of casein micelle dispersions at 12 °C and 42 °C probed by in situ SAXS. *Journal of Membrane Science, 618*, Article 118700. https://doi.org/10.1016/j.memsci.2020.118700

France, T. C., Kelly, A. L., Crowley, S. V., & O'Mahony, J. A. (2021). The effects of temperature and transmembrane pressure on protein, calcium and plasmin partitioning during microfiltration of skim milk. *International Dairy Journal, 114*, Article 104930. https://doi.org/10.1016/j.idairyj.2020.104930

Gaucheron, F., Famelart, M. H., Mariette, F., Raulot, K., Michel, F., & Le Graet, Y. (1997). Combined effects of temperature and high-pressure treatments on physicochemical characteristics of skim milk. *Food Chemistry, 59*(3), 439–447. https://doi.org/10.1016/S0308-8146(96)00303-2

Gebhardt, R., Doster, W., & Kulozik, U. (2005). Pressure-induced dissociation of casein micelles: Size distribution and effect of temperature. *Brazilian Journal of Medical and Biological Research, 38*(8), 1209–1214. https://doi.org/10.1590/S0100-879X2005000800008

Granger-Delacroix, M., Leconte, N., Grassin, C., Le Goff, F., Garnier-Lambrouin, F., Van Audenhaege, M., & Gésan-Guiziou, G. (2023). Skimmed milk microfiltration in diafiltration mode: Impact of solvent nature and concentration factor on spiral-wound membrane performance operated at low temperature. *Separation and Purification Technology, 304*, Article 122326. https://doi.org/10.1016/j.seppur.2022.122326

Hartinger, M., Heidebrecht, H. J., Schiffer, S., Dumpler, J., & Kulozik, U. (2019). Milk protein fractionation by means of spiral-wound microfiltration membranes: Effect of the pressure adjustment mode and temperature on flux and protein permeation. *Foods, 8*(6), 1–17. https://doi.org/10.3390/foods8060180

Hartinger, M., Napiwotzki, J., Schmid, E. M., Hoffmann, D., Kurz, F., & Kulozik, U. (2020). Influence of spacer design and module geometry on the filtration performance during skim milk microfiltration with flat sheet and spiral-wound membranes. *Membranes, 10*(4). https://doi.org/10.3390/membranes10040057

Hartinger, M., Schiffer, S., Heidebrecht, H., Dumpler, J., & Kulozik, U. (2019). Investigation on the spatial filtration performance in spiral-wound membranes – influence and length-dependent adjustment of the transmembrane pressure. *Journal of Membrane Science, 591*, Article 117311. https://doi.org/10.1016/j.memsci.2019.117311

Holdich, R., Schou, K., Dragosavac, M., Kellet, S., & Bandulasena, H. (2018). A comparison of azimuthal and axial oscillation microfiltration using surface and matrix types of microfilters with a cake-slurry shear plane exhibiting non-Newtonian behaviour. *Journal of Membrane Science, 550*, 357–364. https://doi.org/10.1016/j.memsci.2017.12.079

Kattan, O., Ebbers, K., Koolaard, A., Vos, H., & Bargeman, G. (2018). Membrane contactors: An alternative for de-aeration of salt solutions? *Separation and Purification Technology, 205*, 231–240. https://doi.org/10.1016/j.seppur.2018.05.038

Li, X., Mo, Y., Li, J., Guo, W., & Ngo, H. H. (2017). In-situ monitoring techniques for membrane fouling and local filtration characteristics in hollow fiber membrane processes: A critical review. *Journal of Membrane Science, 528*(January), 187–200. https://doi.org/10.1016/j.memsci.2017.01.030

Liang, S. (2016). Performance modeling and analysis of a hollow fiber membrane system. *Journal of Membrane Science & Technology, 6*(1), 1–8. https://doi.org/10.4172/2155-9589.1000144

Marella, C., Sunkesula, V., Hammam, A. R. A., Kommineni, A., & Metzger, L. E. (2021). Optimization of spiral-wound microfiltration process parameters for the production of micellar casein concentrate. *Membranes, 11*(9), 13–16. https://doi.org/10.3390/membranes11090656

Mercier-Bouchard, D., Benoit, S., Doyen, A., Britten, M., & Pouliot, Y. (2017). Process efficiency of casein separation from milk using polymeric spiral-wound microfiltration membranes. *Journal of Dairy Science, 100*(11), 8838–8848. https://doi.org/10.3168/jds.2017-13015

Montagnaro, F. (2024). Sherwood (Sh) number in chemical engineering applications—a brief review. *Energies, 17*(17). https://doi.org/10.3390/en17174342

Ng, K. S. Y., Dunstan, D. E., & Martin, G. J. O. (2018). Influence of diafiltration on flux decline during skim milk ultrafiltration. *International Dairy Journal, 87*, 67–74. https://doi.org/10.1016/j.idairyj.2018.07.021

Nyambura, H. L., Janssen, A. E. M., van der Padt, A., & Boom, R. M. (2025). A geometric model to predict protein retentions during skim milk microfiltration. *Journal of Membrane Science, 722*, Article 123865. https://doi.org/10.1016/j.memsci.2025.123865

Piry, A., Kühnl, W., Grein, T., Tolkach, A., Ripperger, S., & Kulozik, U. (2008). *Length dependency of flux and protein permeation in crossflow microfiltration of skimmed milk* (Vol.325, pp. 887–894). https://doi.org/10.1016/j.memsci.2008.09.025

Reitmaier, M., Bachmann, I., Heidebrecht, H., & Kulozik, U. (2021). Effect of changes in ionic composition induced by different diafiltration media on deposited layer properties and separation efficiency in milk protein fractionation by microfiltration. *International Dairy Journal, 120*, Article 105089. https://doi.org/10.1016/j.idairyj.2021.105089

Renhe, I. R. T., Zhao, Z., & Corredig, M. (2019). A comparison of the heat stability of fresh milk protein concentrates obtained by microfiltration, ultrafiltration and diafiltration. *Journal of Dairy Research, 86*(3), 347–353. https://doi.org/10.1017/S0022029919000426

Rizki, Z., Janssen, A. E. M., Boom, R. M., & van der Padt, A. (2019). Oligosaccharides fractionation cascades with 3 outlet streams. *Separation and Purification Technology, 221*, 183–194. https://doi.org/10.1016/j.seppur.2019.03.086

Samuelsson, G., Dejmek, P., Trägårdh, G., & Paulsson, M. (1997). Minimizing whey protein retention in cross-flow microfiltration of skim milk. *International Dairy Journal, 7*(4), 237–242. https://doi.org/10.1016/S0958-6946(97)00009-5

Samuelsson, G., Huisman, I. H., Trägårdh, G., & Paulsson, M. (1997). Predicting limiting flux of skim milk in crossflow microfiltration. *Journal of Membrane Science, 129*(2), 277–281. https://doi.org/10.1016/S0376-7388(97)00013-6

Schopf, R., & Kulozik, U. (2021). Impact of feed concentration on milk protein fractionation by hollow fiber microfiltration membranes in diafiltration mode. *Separation and Purification Technology, 276*, Article 119278. https://doi.org/10.1016/j.seppur.2021.119278

Schopf, R., Schmidt, F., & Kulozik, U. (2020). Impact of hollow fiber membrane length on the milk protein fractionation. *Journal of Membrane Science.* , Article 118834. https://doi.org/10.1016/j.memsci.2020.118834

Schopf, R., Schmidt, F., Linner, J., & Kulozik, U. (2021). Comparative assessment of tubular ceramic, spiral wound, and hollow fiber membrane microfiltration module systems for milk protein fractionation. *Foods, 10*(4). https://doi.org/10.3390/foods10040692

Song, B., Zhang, Y., Lu, J., Pang, X., Wei, M., Zheng, S., Zhang, M., Zhang, S., & Lv, J. (2021). Effect of different diafiltration process on the protein fractionation of skim milk by cross flow microfiltration. *Food Science and Technology, 152*, Article 112330.

Steinhauer, T., Hanély, S., Bogendörfer, K., & Kulozik, U. (2015). Temperature dependent membrane fouling during filtration of whey and whey proteins. *Journal of Membrane Science, 492*, 364–370. https://doi.org/10.1016/j.memsci.2015.05.053

Steinhauer, T., Kühnl, W., & Kulozik, U. (2011). Impact of protein interactions and transmembrane pressure on physical properties of filter cakes formed during filtrations of skim milk. *Procedia Food Science, 1*, 886–892. https://doi.org/10.1016/j.profoo.2011.09.134

Tan, T. J., Wang, D., & Moraru, C. I. (2014). A physicochemical investigation of membrane fouling in cold microfiltration of skim milk. *Journal of Dairy Science, 97*(8), 4759–4771. https://doi.org/10.3168/jds.2014-7957

Tremblay-Marchand, D., Doyen, A., Britten, M., & Pouliot, Y. (2016). A process efficiency assessment of serum protein removal from milk using ceramic graded permeability microfiltration membrane. *Journal of Dairy Science, 99*(7), 5230–5243. https://doi.org/10.3168/jds.2016-10914

Vadi, P. K., & Rizvi, S. S. H. (2001). Experimental evaluation of a uniform transmembrane pressure crossflow microfiltration unit for the concentration of micellar casein from skim milk. *Journal of Membrane Science, 189*(1), 69–82. https://doi.org/10.1016/S0376-7388(01)00396-9

Wang, C. Y., Mercer, E., Kamranvand, F., Williams, L., Kolios, A., Parker, A., Tyrrel, S., Cartmell, E., & McAdam, E. J. (2017). Tube-side mass transfer for hollow fibre membrane contactors operated in the low Graetz range. *Journal of Membrane Science, 523*, 235–246. https://doi.org/10.1016/j.memsci.2016.09.049

Yeh, H. M. (2009). Exponential model analysis of permeate flux for ultrafiltration in hollow-fiber modules by momentum balance. *Chemical Engineering Journal, 147*(2–3), 202–209. https://doi.org/10.1016/j.cej.2008.07.002

Zulewska, J., & Barbano, D. M. (2013). Influence of casein on flux and passage of serum proteins during microfiltration using polymeric spiral-wound membranes at 50°C. *Journal of Dairy Science, 96*(4), 2048–2060. https://doi.org/10.3168/jds.2012-6032

Zulewska, J., Newbold, M., & Barbano, D. M. (2009). Efficiency of serum protein removal from skim milk with ceramic and polymeric membranes at 50°C. *Journal of Dairy Science, 92*(4), 1361–1377. https://doi.org/10.3168/jds.2008-1757